Pathways for H_2O Bend Vibrational Relaxation in Liquid Water

Rossend Rey*

Departament de Física i Enginyeria Nuclear, Universitat Politècnica de Catalunya, Campus Nord B4−B5, Barcelona 08034, Spain

Francesca Ingrosso†

Equipe de Chimie et Biochimie Théoriques UMR 7565 SRSMC - CNRS, Nancy Université, Boulevard des Aiguillettes BP 70239, 54506 Vandoeuvre-lès-Nancy Cedex, France

Thomas Elsaesser‡

Max-Born-Institut für Nichtlineare Optik und Kurzzeitspektroskopie, Max Born Strasse 2A, D-12489 Berlin, Germany

James T. Hynes§

Department of Chemistry and Biochemistry University of Colorado, Boulder, Colorado 80309-0215, and Chemistry Department, Ecole Normale Supérieure, and Centre National de la Recherche Scientifique Unité Mixte de Recherche 8640, 24 Rue Lhomond, 75005 Paris, France

Received: April 20, 2009; Revised Manuscript Received: June 5, 2009

The mechanism of the H_2O bend vibrational relaxation in liquid water has been examined via classical MD simulations and an analysis of work and power contributions. The relaxation is found to be dominated by energy flow to the hindered rotation of the bend excited water molecule. This energy transfer, representing approximately 2/3 of the transferred energy, is due to a 2:1 Fermi resonance for the centrifugal coupling between the water bend and rotation. The remaining energy flow (∼1/3) from the excited water bend is dominated by transfer to the excited water molecule's first four water neighbors, i.e., the first hydration shell, and is itself dominated by energy flow to the two water molecules hydrogen (H)-bonded to the hydrogens of the central H_2O. The energy flow from the produced rotationally excited central molecule is less local in character, with approximately half of its rotational kinetic energy being transferred to water molecules outside of the first hydration shell, whereas the remaining half is preferentially transferred to the two first hydration shell water molecules donating H-bonds to the central water oxygen. The overall energy flow is well described by an approximate kinetic scheme.

I. Introduction

In a recent contribution[1] (hereafter I), we have examined, via nonequilibrium classical molecular dynamics (MD) simulations, the time scale and energy flow pathway for the relaxation of an excited H_2O bend vibration in liquid water, together with the related issues for the decay of librational (hindered rotational) H_2O energy. The time scale for the bend relaxation was found to be ∼270 fs, in reasonable agreement with ultrafast infrared (IR) measures (∼170 − 260 fs) for the H_2O bend in liquid H_2O.[2−7] The H_2O librational energy decay time scale, more precisely that of the librational kinetic energy, was found to be ∼30 fs, consistent with the experimental[2,3] upper bound ∼100 fs.[8] In addition to these time scales, the energy flow pathway for the relaxation of the water bend vibration was followed through the first several hydration shells of the excited water, as was (in separate calculations) the relaxation of a rotationally excited water molecule. In addition to the quite rapid energy flow through these shells, the most striking feature of the flow patterns found in I was the significant contribution of a rapid initial intramolecular water bend to water rotation energy transfer.

There are however several limitations for this previous study. First, in order to render the energy flow route visible, considerable initial excitation was required, e.g., an energy corresponding to approximately three quanta of the water bend. Since experimentally it is the bend fundamental that is involved,[2,3] it is desirable to establish the flow pattern at a lower level of excitation. Second, although a 2:1 Fermi resonance[1,9,10] for the centrifugal coupling[1,11,12] between the excited water bend and (hindered) rotation was strongly implicated for the important intramolecular bend to rotation energy transfer, this was not explicitly established in I. Third, while energy transfer to the first hydration shell of the excited water was followed, no distinction could be made between the roles of different water molecules in that shell, e.g., those receiving and those donating hydrogen bonds to the excited water molecule.

In the present work, we examine the water bend relaxation problem in a different fashion. In particular, we employ the power and work formulation introduced for vibrational energy relaxation by Whitnell et al.[11,13] and employed in various

* To whom correspondence should be addressed. Electronic address: rosendo.rey@upc.edu.
† Electronic address: Francesca.Ingrosso@cbt.uhp-nancy.fr.
‡ Electronic address: elsasser@mbi-berlin.de.
§ Electronic address: hynes@spot.colorado.edu.

10.1021/jp9036342 CCC: $40.75
Published on Web 07/13/2009

subsequent studies.[14] This formulation, in connection with nonequilibrium MD trajectory studies, enables us to clearly expose the energy flow pathway for the water bend fundamental, including the crucial participation of the excited water's rotation, whose centrifugal coupling[1,11,12] to the water bend is here shown to give a near-resonant 2:1 Fermi resonance[1,9,10] in aqueous solution. The key inertial axis rotation of the water molecule is also identified. The formulation also allows a clear picture of the participation of the water molecules in the excited water's first hydration shell, and their dependence on their hydrogen bonding character vis a vis the excited water molecule. Further, the formulation permits clarification of the role of different hydration shells in the relaxation of the rotational energy received by the bend excited water via the centrifugal coupling.

We add a brief remark concerning nomenclature. Any rotation of a water molecule in the liquid is hindered, i.e., librational in character. Since within we will be primarily concerned with rotational kinetic energy and a "libration" actually refers to both kinetic and potential energy aspects, hereafter we generally employ the terms "rotation" or "rotational'.

The outline of the remainder of this paper is as follows. In section II, we present the basic theoretical formulation, focusing especially on the definitions of the power and the work associated with the excited water bend vibration and the hindered rotation of that same water molecule. The basic scheme for the stages of, and contributions to, the energy flow is also introduced here. The computational details are given in section III. The power and work results are presented in section IV, where the importance of the Fermi resonance centrifugal coupling between the water bend and rotation is demonstrated, as is the participation of different first hydration shell water molecules in the energy flow directly from the excited water's bend vibration as well as from that water's induced rotational excitation. A simplified kinetic scheme is shown in section V to well describe the results. Concluding remarks are offered in section VI.

II. Theoretical Formulation

A. Model. The model we employ for the bend excited water molecule is the same as in I,[1] namely a SPC/E[15] molecule in which only the intramolecular bending is allowed to vibrate, with the O−H distances kept fixed at their equal equilibrium value R. (All of the other molecules in the problem are taken to be rigid). Since there is only one vibrational mode, a number of important quantities can be worked out analytically, which will greatly simplify the analysis. We begin with the water molecule coordinates. The Eckart configuration (which allows for an optimum separation of rotation and vibration) corresponding to a given distorted configuration can be easily shown[16] to be the one displayed in Figure 1. Since the OH bonds have a fixed length R, the position vectors in the bending plane can be written in terms of the instantaneous bend angle (θ) between the OH bonds

$$\begin{aligned}\vec{r}_{\mathrm{O}} &= \left(0, 2\frac{m_H}{M}R\cos\left(\frac{\theta}{2}\right)\right)\\ \vec{r}_{\mathrm{H1}} &= \left(R\sin\left(\frac{\theta}{2}\right), -\frac{m_O}{M}R\cos\left(\frac{\theta}{2}\right)\right)\\ \vec{r}_{\mathrm{H2}} &= \left(-R\sin\left(\frac{\theta}{2}\right), -\frac{m_O}{M}R\cos\left(\frac{\theta}{2}\right)\right)\end{aligned} \tag{1}$$

The vibrational velocities are just the derivatives

$$\begin{aligned}\vec{v}_{\mathrm{O}} &= \left(0, -\frac{m_{\mathrm{H}}}{M}R\sin\left(\frac{\theta}{2}\right)\dot{\theta}\right)\\ \vec{v}_{\mathrm{H1}} &= \left(\frac{R}{2}\cos\left(\frac{\theta}{2}\right)\dot{\theta}, \frac{m_{\mathrm{O}}}{2M}R\sin\left(\frac{\theta}{2}\right)\dot{\theta}\right)\\ \vec{v}_{\mathrm{H2}} &= \left(-\frac{R}{2}\cos\left(\frac{\theta}{2}\right)\dot{\theta}, \frac{m_{\mathrm{O}}}{2M}R\sin\left(\frac{\theta}{2}\right)\dot{\theta}\right)\end{aligned} \tag{2}$$

with $\dot{\theta}$ denoting the bend angular velocity. From the antisymmetry of the hydrogen velocities along the x axis, it follows that there will be no vibrational angular momentum and thus the present model does not contain any Coriolis coupling.

Upon writing the bend vibrational kinetic energy (K_{vib}) in terms of these velocities,

$$K_{\mathrm{vib}} = \frac{1}{2}\sum m_i(\vec{v}_i)^2 = \frac{m_{\mathrm{H}}R^2}{2M}(m_{\mathrm{O}} + m_{\mathrm{H}} + m_{\mathrm{H}}\cos\theta)\dot{\theta}^2 \tag{3}$$

we obtain the effective mass for the bend vibration as

$$\mu_{\mathrm{eff}} = \frac{m_{\mathrm{H}}R^2}{M}(m_{\mathrm{O}} + m_{\mathrm{H}} + m_{\mathrm{H}}\cos\theta) \tag{4}$$

where M denotes the total water molecular mass.

B. Hamiltonian. With these preliminaries, we turn to the water molecule Hamiltonian. The Hamiltonian of a classical polyatomic molecule is[17]

$$\begin{aligned}H &= K_{\mathrm{CM}} + K_{\mathrm{rot}} + K_{\mathrm{Coriolis}} + K_{\mathrm{vib}} + U_{\mathrm{pot}}\\ &= \frac{1}{2}M\vec{v}_{\mathrm{CM}}^2 + \frac{1}{2}\sum m_i(\vec{\omega}\times\vec{r}_i)^2 +\\ &\quad \vec{\omega}\cdot\sum m_i(\vec{\rho}_i\times\vec{v}_i) + \frac{1}{2}\sum m_i\vec{v}_i^{\,2} + U_{\mathrm{pot}}\end{aligned} \tag{5}$$

where K_{vib} is the vibrational kinetic energy (eq 3), $\vec{\omega}$ is the angular velocity vector, and $\vec{\rho}_i$ stands for the displacements from

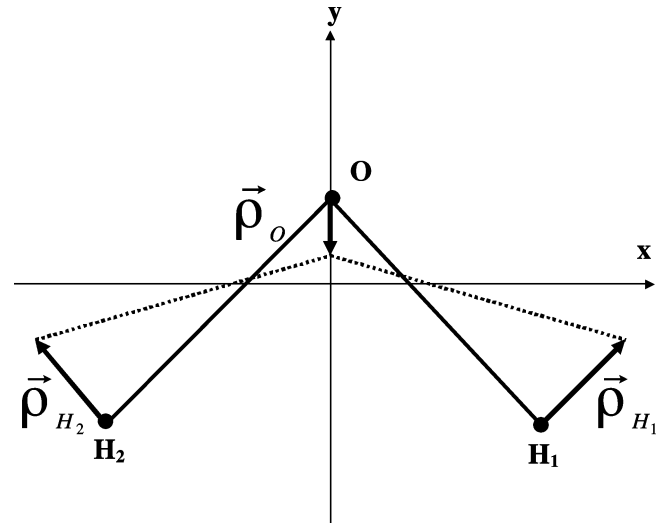

Figure 1. Eckart configuration (dotted line) corresponding to an instantaneous (dotted line) configuration of the water molecule. Also included: axis definitions (centered at the center of mass), and instantaneous displacements with respect to the Eckart configuration. (The y and z axis definitions here differ from those in ref 1).

the Eckart configuration (Figure 1). The corresponding term in the Hamiltonian involving those displacements is the product of $\vec{\omega}$ and the vibrational angular momentum which, as previously discussed, is zero in the present water model, and we are left with

$$H = \frac{1}{2}M\vec{v}_{\mathrm{CM}}^2 + \frac{1}{2}\sum m_i(\vec{\omega}\times\vec{r}_i)^2 + \frac{1}{2}\sum_i m_i\vec{v}_i^{\,2} + \frac{1}{2}k_{\mathrm{b}}(\theta-\theta_{\mathrm{eq}})^2 \quad (6)$$

i.e., the center of mass (CM) kinetic energy, plus the rotational kinetic energy (for which there is no ambiguity in the present model), plus the vibrational energy comprising the last two terms, with the bend potential energy assumed to be harmonic.

The rotational kinetic energy can also be expressed in terms of the water molecule's moment of inertia. The principal values, with respect to the principal axes displayed in Figure 1, are

$$\begin{aligned} I_{xx} &= \frac{2R^2 m_{\mathrm{O}} m_{\mathrm{H}}}{M}\cos^2\!\left(\frac{\theta}{2}\right) \cong 0.6 \\ I_{yy} &= 2m_{\mathrm{H}}R^2\sin^2\!\left(\frac{\theta}{2}\right) \cong 1.3 \\ I_{zz} &= I_{xx} + I_{yy} \cong 1.9 \end{aligned} \quad (7)$$

where the numbers are the approximate values for the equilibrium angle ($\theta_{\mathrm{eq}} = 109.47°$) (in units amu·Å^2).

C. Power. As discussed in the Introduction, the present work relies heavily on the computation of the power exerted on the different (vibrational, rotational, translational) modes, as this allows us to easily pinpoint the paths of the energy flow from the excited water bend vibration.[11] In order to obtain the formula for each power (i.e., the time rate of change of energy), it is only required to take the time derivative of the corresponding term in the Hamiltonian (eq 6).

The simplest case is that of the power (i.e., the time rate of the kinetic energy change) on the translational mode of the water molecule. Differentiating the CM kinetic energy we have

$$\frac{\mathrm{d}K_{\mathrm{CM}}}{\mathrm{d}t} = \frac{\mathrm{d}}{\mathrm{d}t}\left(\frac{1}{2}M\vec{v}_{\mathrm{CM}}^2\right) = \vec{F}_{\mathrm{ext}}\cdot\vec{v}_{\mathrm{CM}} \quad (8)$$

Partitioning the external force $\vec{F}_{\mathrm{ext}}$ in terms of the contributions from each molecule (or groups of molecules of interest) is one example of the feature that allows for the detailed study just referred to. This formula constitutes the simplest illustration of what is also possible for rotational and vibrational modes, although the derivation of the corresponding formulas requires more care, as will now be seen.

Turning to the power for the water bend vibration, we consider first the derivative of the vibrational kinetic energy

$$\frac{\mathrm{d}K_{\mathrm{vib}}}{\mathrm{d}t} = \frac{\mathrm{d}}{\mathrm{d}t}\left(\frac{1}{2}\sum_i m_i\vec{v}_i^{\,2}\right) = \sum_i m_i\vec{v}_i\cdot\frac{\mathrm{d}\vec{v}_i}{\mathrm{d}t} \quad (9)$$

into which we substitute the relation[18] between velocities in the inertial system (denoted with capital letters) and in the Eckart frame (lower case)

$$\frac{\mathrm{d}\vec{v}_i}{\mathrm{d}t} = \frac{\mathrm{d}\vec{V}_i}{\mathrm{d}t} - \dot{\vec{\omega}}\times\vec{r}_i - \vec{\omega}\times(\vec{\omega}\times\vec{r}_i) - 2\vec{\omega}\times\vec{v}_i \quad (10)$$

Only two terms survive

$$\begin{aligned} \frac{\mathrm{d}K_{\mathrm{vib}}}{\mathrm{d}t} &= \sum_i m_i\vec{v}_i\cdot\frac{\mathrm{d}\vec{V}_i}{\mathrm{d}t} - \sum_i m_i\vec{v}_i\cdot\vec{\omega}\times(\vec{\omega}\times\vec{r}_i) \\ &= \sum_i \vec{F}_i^{\mathrm{tot}}\cdot\vec{v}_i - \sum_i m_i\vec{v}_i\cdot\vec{\omega}\times(\vec{\omega}\times\vec{r}_i), \end{aligned} \quad (11)$$

where the first term is just the total power coming from forces, both internal and external, and the second term arises from centrifugal coupling. After some algebraic manipulation, the latter term can be expressed in terms of the components of the angular velocity in the Eckart coordinate system

$$\frac{\mathrm{d}K_{\mathrm{vib}}}{\mathrm{d}t} = \sum_i \vec{F}_i^{\mathrm{tot}}\cdot\vec{v}_i - \frac{m_{\mathrm{H}}R^2\sin\theta}{2M}(m_{\mathrm{O}}\omega_x^2 - M\omega_y^2 - 2m_{\mathrm{H}}\omega_z^2)\dot{\theta} \quad (12)$$

The bend vibrational power is completed with the time derivative of the vibrational potential energy, for which we have

$$\frac{\mathrm{d}U_{\mathrm{vib}}}{\mathrm{d}t} = \sum_i \frac{\mathrm{d}U_{\mathrm{vib}}}{\mathrm{d}\vec{r}_i}\cdot\vec{V}_i = -\sum_i \vec{F}_i^{\mathrm{int}}\cdot\vec{V}_i = -\sum_i \vec{F}_i^{\mathrm{int}}\cdot\vec{v}_i \quad (13)$$

with the last equality resulting from the inertial-Eckart frame velocity relation $\vec{V}_i = \vec{v}_i + \vec{\omega}\times\vec{r}_i$, and involving the intramolecular force.

Combination of eqs 12 and 13 gives the derivative of the total vibrational energy

$$\frac{\mathrm{d}E_v}{\mathrm{d}t} = \frac{\mathrm{d}K_{\mathrm{vib}}}{\mathrm{d}t} + \frac{\mathrm{d}U_{\mathrm{vib}}}{\mathrm{d}t} = \sum_i \vec{F}_i^{\mathrm{tot}}\cdot\vec{v}_i - \sum_i \vec{F}_i^{\mathrm{int}}\cdot\vec{v}_i - \frac{m_{\mathrm{H}}R^2\sin\theta}{2M}(m_{\mathrm{O}}\omega_x^2 - M\omega_y^2 - 2m_{\mathrm{H}}\omega_z^2)\dot{\theta} \quad (14)$$

from which follows the power formula we will use in the calculations

$$P_{\mathrm{vib}}(t) \equiv \frac{\mathrm{d}E_v}{\mathrm{d}t} = \sum_i \vec{F}_i^{\mathrm{ext}}\cdot\vec{v}_i - \frac{m_{\mathrm{H}}R^2\sin\theta}{2M}(m_{\mathrm{O}}\omega_x^2 - M\omega_y^2 - 2m_{\mathrm{H}}\omega_z^2)\dot{\theta} \equiv P_{\mathrm{vib}}^{\mathrm{ext}}(t) + P_{\mathrm{vib}}^{\mathrm{VR}}(t) \quad (15)$$

i.e., the total power on the vibrational mode ($P_{\mathrm{vib}}(t)$) results from the sum of the power associated with the external forces $P_{\mathrm{vib}}^{\mathrm{ext}}(t)$ (which, again, can be partitioned into the different contributions), and the power resulting from centrifugal vibration−rotation (VR) coupling $P_{\mathrm{vib}}^{\mathrm{VR}}(t)$.

We now turn to the power for the water rotational kinetic energy, i.e., the time derivative of the rotational kinetic energy. In this power, the term $P_{\mathrm{vib}}^{\mathrm{VR}}(t)$ in eq 15 must also appear, with the opposite sign. To evaluate the time deriva-

tive, we employ the principal axes and their associated angular velocities

$$\frac{dK_R}{dt} = \frac{d}{dt}\left(\frac{1}{2}\sum_\alpha I_\alpha \omega_\alpha^2\right) = \frac{1}{2}\sum_\alpha \frac{dI_\alpha}{dt}\omega_\alpha^2 + \sum_\alpha I_\alpha \omega_\alpha \frac{d\omega_\alpha}{dt} \tag{16}$$

This can be re-expressed in terms of the angular momentum components time derivative

$$\frac{dL_\alpha}{dt} = \frac{dI_\alpha}{dt}\omega_\alpha + I_\alpha \frac{d\omega_\alpha}{dt} \tag{17}$$

so that

$$\frac{dK_R}{dt} = \sum_\alpha \frac{dL_\alpha}{dt}\omega_\alpha - \frac{1}{2}\sum_\alpha \frac{dI_\alpha}{dt}\omega_\alpha^2 \tag{18}$$

where the first term is just the power associated with the external torque, with components $(\tau_{ext})_\alpha = dL_\alpha/dt$, and the second term arises from the vibration−rotation centrifugal coupling. After computing the derivatives of the inertia moment components (see eq 7), this term indeed turns out to be the same as we obtained in the derivative of the vibrational energy, but with opposite sign. The rotational power is thus given by

$$P_R(t) \equiv \frac{dK_R}{dt} = \vec{\tau}_{ext}\cdot\vec{\omega} + \frac{m_H R^2 \sin\theta}{2M}(m_O\omega_x^2 - M\omega_y^2 - 2m_H\omega_z^2)\dot{\theta} \equiv P_R^{ext}(t) + P_R^{VR}(t) \tag{19}$$

where now it is the torque $(\vec{\tau}_{ext})$ which can be partitioned into the contributions of choice.

D. Work. With the power formulas developed above, we can compute the total amount of energy that flows from some specific mode of a given molecule into another molecule (or group of molecules). We recall for instance that eq 15 shows that there are two contributions to the water bend vibrational energy variation

$$\frac{dE_v}{dt} = P_{vib}^{ext} + P_{vib}^{VR} \tag{20}$$

so that, after time integration, the time-dependent change in bend vibrational energy will be expressed in terms of the time-integrated power contributions of work performed during the process

$$E_v(t) - E_v(0) \equiv \Delta E_v(t) = \int_0^t P_{vib}^{ext}\,dt + \int_0^t P_{vib}^{VR} \equiv W_{ext}(t) + W_{VR}(t) \tag{21}$$

If we consider a nonequilibrium simulation, with the water molecule's bend vibrationally excited at the initial time, by the end of the relaxation process these work contributions will plateau at certain values that will add up to (minus) the initial excess energy. On the other hand, in the case of equilibrium simulations, only the power contributions will be of interest, as the total work will average to zero.

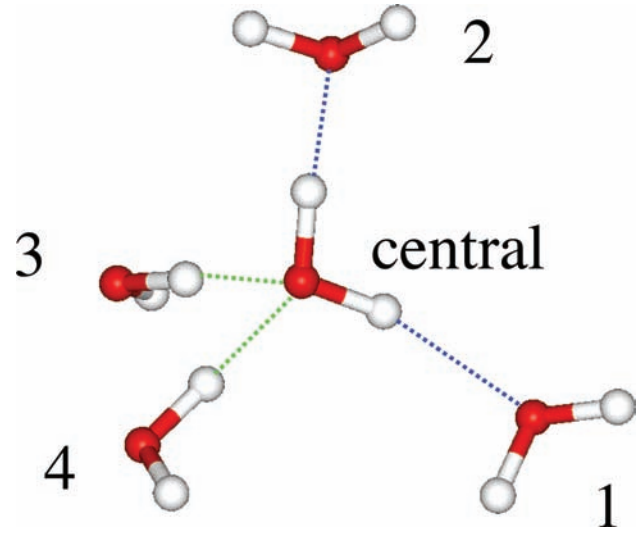

Figure 2. Sketch of the numbering of molecules around the "central" (bend excited) water molecule. The two water molecules directly H-bonded (blue dotted lines) to the hydrogens of the excited water molecule are referred as 1 and 2, while the other two waters donating H-bonds (green dotted lines) to the excited water are referred as 3 and 4.

We will pursue the same basic approach for the work done on the rotation and translation of the bend vibrationally excited water molecule (eqs 8 and 19), and on the rotation and translation of the immediate neighbors of this excited water. For these first hydration shell water molecules, there is no vibration, since these are treated as rigid molecules. Furthermore, we will partition this group of four immediate neighbors into two subsets: the two water molecules directly hydrogen (H)-bonded to the hydrogens of the excited water molecule will be referred as 1 and 2 (or 12 when considered as a group), and the other two waters donating H-bonds to the excited water will be referred as 3 and 4 (34 as a group), see Figure 2. (This differs from the division into two hydration shells and the bulk made in I).

Since it will be necessary to keep track of a substantial number of different work contributions, they will henceforth be labeled with the notation $W_i^{\alpha(j)}$, where i denotes the molecule (or molecules) doing the work, and α the mode of molecule j on which this work is done (i.e., $W_{12}^{V(C)}$ would refer to the work done by molecules 1 and 2 on the bend vibration (V) of the central (C) molecule).

This approach allows for a rather detailed, and potentially complex, analysis of the energy flow from the bend vibrationally excited water molecule. In order to obtain a picture that captures the basic features of this flow, the contributions to the work performed on the excited molecule have been partitioned in the fashion illustrated in Figure 3. We distinguish, with subsequent justification, two stages in the process: a "first stage" in which the excited water's bend vibrational energy directly flows into its neighbors (W_{ext}, with the subscript indicating "external" to the bend excited water molecule), and also flows into this water's own rotation (W_{VR}), and a "second stage" in which this excess rotational energy flows into the rotations and translations of the neighbors of the central, excited water.

Furthermore, each of the two contributions to the work performed by water molecules external to the central, bend excited water (i.e., the work on the central water's bend vibrational mode and the work on the central water's rotational mode) has been partitioned into three contributions: that of water

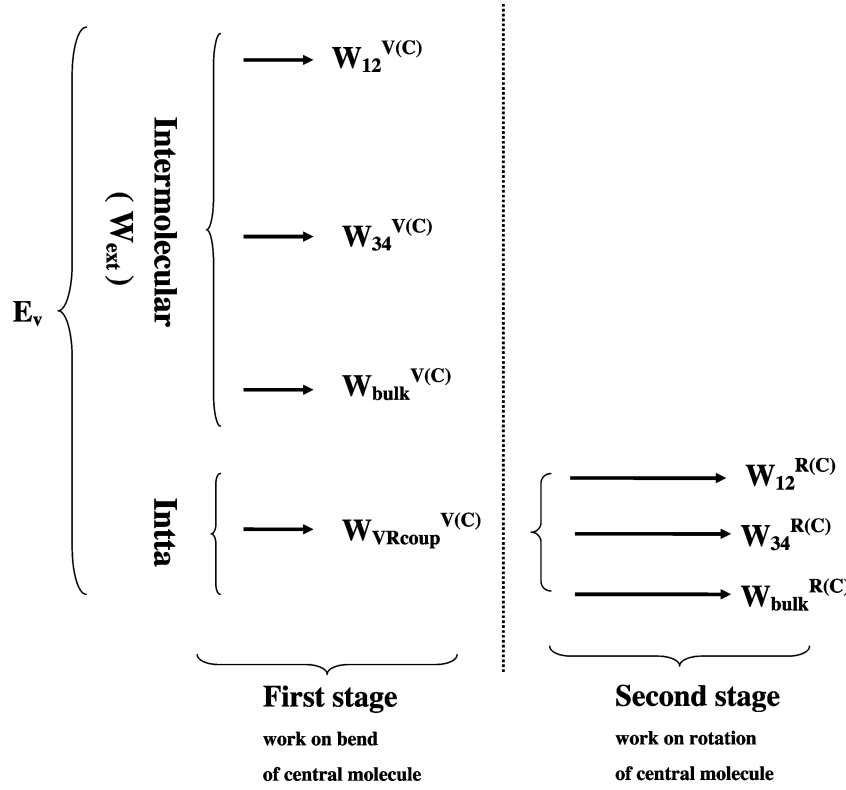

Figure 3. Different contributions to the work exerted on the bend vibrationally excited water molecule, computed in this work. There are two basic contributions: intermolecular, i.e., work done by the rest of the liquid on the excited, central water; and intramolecular, i.e., that coming from centrifugal coupling and which thus produces rotation of the central water. Notice that the external work on the water bend vibration has been partitioned into three contributions (that of water molecules 1 and 2; that of water molecules 3 and 4 (see Figure 2); and that of the rest of the liquid). The same partitioning has been used for the work on the central water's rotation.

molecules 1 and 2, that of water molecules 3 and 4, and that of the rest of the liquid, i.e., beyond the first hydration shell. We have for instance that the external work on the central water vibrational mode is expressed as

$$W_{\text{ext}} = W_{12}^{\text{V(C)}} + W_{34}^{\text{V(C)}} + W_{\text{bulk}}^{\text{V(C)}} \qquad (22)$$

reflecting our a priori expectation that the first stage energy flow process will be mainly local in character (and thus that the central water's first four neighbors will be particularly relevant), and that these four molecules will not have an equivalent role (one might expect that molecules 1 and 2 H-bonded to the central bend-excited water's hydrogens might play the leading role). A similar formula holds for the work on the central water molecule's rotation ("second stage", see Figure 3).

III. Computational Details

A. Model. The SPC/E model[15] has been adopted for the water molecules. All simulations have been run with an in-house code using 200 molecules, with a time step of 1 fs, at a mean temperature of 300 K, with a box size of 18.15 Å, and with a cutoff distance of 8.57 Å. The Ewald sum correction has been included for Coulomb forces. As stated in section II.A, the bending mode of one of the molecules is allowed to vibrate (in all nonequilibrium and some equilibrium simulations, see below) with a force constant of 90.45 kcal/mol.[1] This force constant corresponds to a water bend frequency of 1660 cm^{-1} that is close to the experimental value of 1650 cm^{-1}.

Three sets of simulations have been carried out:

• Equilibrium simulations with all water molecules rigid, in order to compute rotational energy time correlation functions (total and around the different body centered axes) and the corresponding Fourier transforms. The equations of motion have been integrated with a leapfrog algorithm[19] that involves temperature control, with internal constraints handled with the "SHAKE" algorithm.[20]

• Equilibrium simulations with all water molecules rigid except one, in order to determine equilibrium time-dependent values of the powers exerted on different modes.

• Nonequilibrium simulations. A long trajectory with all water molecules kept rigid is integrated in a fashion similar to the equilibrium simulations described above. Every 2 ps the instantaneous configuration is taken as the initial one for a nonequilibrium run. A bending angle is sampled for one of the water molecules (see the next subsection for further details) and a bend velocity is added so that a total energy $^3/_2\hbar\omega_b$ is put into the bending mode,[21] where ω_b is the harmonic bend frequency. This water's translational and rotational velocities are kept without changes, which can result in slightly larger or smaller rotational kinetic energy depending on whether the angle sampled is larger or smaller than the equilibrium value. No resampling of rotational/translational velocities has been done for the remaining molecules. The nonequilibrium trajectory is run for 3 ps without temperature control, while the quantities to be analyzed (energy, power, work) are computed. Most of the results to be described correspond to a total of 2000 trajectories, although smaller sets have been used as well to assess the effect of initial conditions. Equations of motion for the nonequilibrium trajectories have been integrated with the "RATTLE" algorithm.[22]

B. Initial Conditions. Since at the initial time of the nonequilibrium simulations the water molecule is distorted from the equilibrium configuration (with bend angle increments that

can reach up to 20° from the equilibrium value, see below), we have assessed the possible effect that the probability distribution assumed for this increment might have on the final results. Three different sets of probability distributions have been tested:

• Thermal. Here the angle increment is sampled according to a thermal distribution, assuming that we approximately have a harmonic oscillator with a constant effective mass μ (in our model the potential energy is exactly harmonic and the effective mass, eq 4, has only a feeble dependence on angle). The distribution in this case is just a Gaussian, and thus peaks at zero

$$p_{\text{thermal}} = \sqrt{\frac{\mu\omega_b^2}{2\pi k_B T}} e^{-\mu\omega_b^2\theta^2/2k_B T} \tag{23}$$

• Quantum. In addition to the addition of an initial energy of $^3/_2\hbar\omega_b$ to the water bend vibration, one could try to mimic the probability distribution of angles in the first excited state, a distribution substantially different from the previous one (with two relative maxima and a zero at the center). In this case, the corresponding distribution is (again for a harmonic oscillator)

$$p_{\text{quantum}} = \sqrt{\frac{2}{\pi}}\left(\frac{\mu\omega_b}{\hbar}\right)^{3/2}\theta^2 e^{-\mu\omega_b\theta^2/\hbar} \tag{24}$$

It should however be remarked that it will not be possible to sample the full distribution, as the tails correspond to angles beyond those classically allowed by the bend potential energy.

• Equiprobable phase. In their study of vibrational relaxation in bromoform using classical dynamics,[21] Ramesh and Sibert sample from an equiprobable distribution of phase in an action-angle treatment of the oscillator.[24] This approach is based on the feature that both position and momentum of the oscillator can be written in terms of a phase (α). In the approximation of a harmonic oscillator

$$\begin{aligned} \theta &= \sqrt{\frac{2E}{\mu\omega_b^2}}\sin\alpha \\ p_\theta &= \sqrt{2\mu E}\cos\alpha \end{aligned} \tag{25}$$

which can be used to produce a probability distribution for θ. With the assumption of a uniform distribution for α ($p_\alpha = 1/2\pi$)

$$p_\alpha d\alpha = p_\alpha(\alpha(\theta))\frac{d\alpha}{d\theta}d\theta = \frac{1}{2\pi}\frac{1}{\sqrt{\frac{2E}{\mu\omega_b^2} - \theta^2}}d\theta \tag{26}$$

so that finally

$$p_{\text{phase}} = \frac{1}{2\pi}\frac{1}{\sqrt{\frac{2E}{\mu\omega_b^2} - \theta^2}} \tag{27}$$

This distribution clearly shows the classical turning points for the bending angle ($\theta_{\max} = \sqrt{2E/\mu\omega_b^2} \approx 20°$). Almost all the results that we report correspond to this case although, as will be shown, no significant differences result from using any of the three probability distributions.

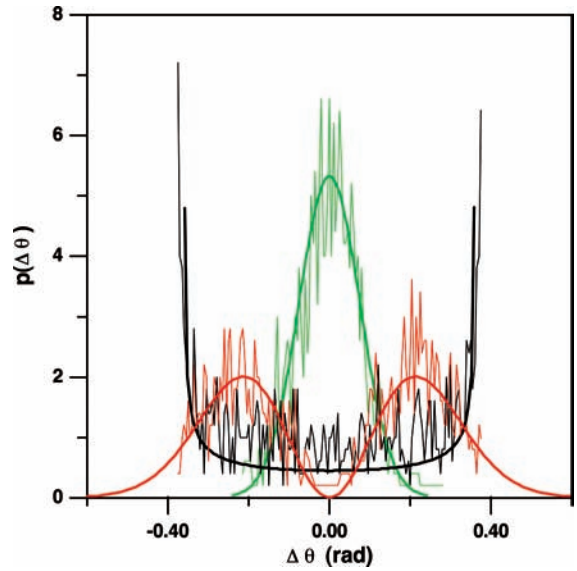

Figure 4. Distributions of initial water bend angle obtained from a sampling of 1000 trajectories. Thin lines correspond to the actual sampling and thick ones to theoretical curves described in the text. Green corresponds to the "thermal" distribution, black to "equiprobable phase", and red to "quantum" (note that for this case the nonclassical tails are not sampled). The x axis corresponds to the deviation from equilibrium angle measured in rad.

Figure 4 displays the actual distributions of initial angles obtained for 1000 trajectory runs. The thin lines correspond to the actual sampling and the thick ones to theoretical curves (note that for the quantum case the classically forbidden distribution tails are not sampled).

IV. Results

A. Equilibrium Results. In order to gain some initial insight into the energy flow from the excited water bend viewed from the present perspective of power and work (as opposed to the monitoring of excess energies in each mode that was done in I), we start by examining at the results from equilibrium simulations where the bend of one of the water molecules is allowed to vibrate. As noted in section II.D, in this setting it is only the power which is of interest, as the work averages to zero.

Figure 5 displays the results for a time span of 0.5 ps. The feature which stands out at the outset is that most of the power is accounted for by the four immediate neighbors in the first hydration shell of the bending water. Indeed the power associated with these four waters tends to be larger than the total power, implying that the rest of the liquid compensates for this slightly larger amount. This result supports our a priori notion that the process of intermolecular energy transfer, from vibration to rotational/translational modes (and vice versa), is largely local. Indeed (not shown) the main contribution comes from the two molecules H-bonded to the hydrogens of the central flexible one (denoted 1 and 2; see Figure 2). In addition, we note that the power associated with the intramolecular centrifugal coupling is comparatively almost negligible, so that the pathway of energy transfer from bending to self-rotation appears to be rather inefficient.

On the basis of these equilibrium results, it would seem reasonable to expect that for nonequilibrium trajectories most, if not all, of the water bend vibrational excess energy, will go

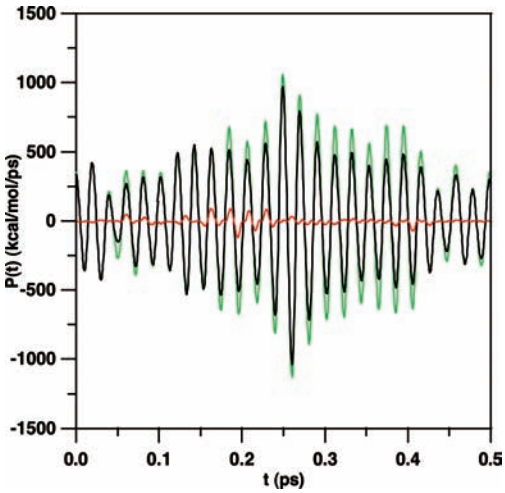

Figure 5. Contributions to the power exerted on the central water's bend vibrational mode. Black line: total power exerted by external forces, i.e., by all other water molecules, P_{vib}^{ext} (see eq 15); green: contribution to this power coming from the central water's four closest water neighbors (the first hydration shell); red: power coming from centrifugal coupling between the central water's bend and rotation, P_{vib}^{VR} (see eq 15).

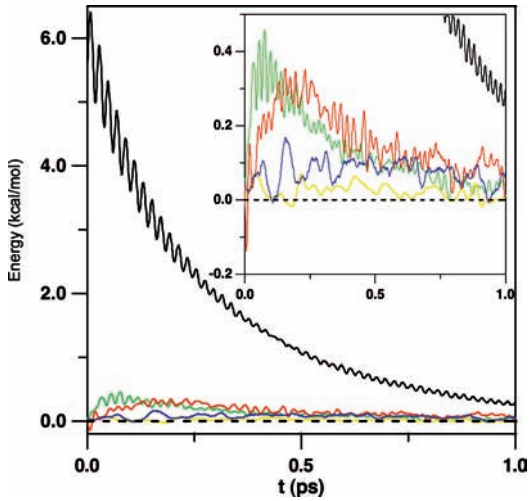

Figure 6. Averaged excess energy in each of the modes for trajectories in which the bend of one of the water molecules is initially excited. Black: vibrational energy of initially excited H_2O; green: rotational kinetic energy of this same molecule; red: rotational kinetic energy of its immediate four neighbors combined; yellow: translational kinetic energy of the vibrationally excited molecule; blue: translational kinetic energy of the immediate four water neighbors combined. The inset displays a blow up of rotational/translational excess energy.

into rotational/translational motions of the four immediate water neighbors, with molecules 1 and 2 taking a higher proportion, and with a marginal flow of energy into self-rotation. But the latter conclusion is strongly at odds with the conclusions of I, and further analysis is clearly called for.

B. Nonequilibrium Results: Energy. In order to ascertain whether the expectation suggested by the above equilibrium results is correct, we now turn to the nonequilibrium simulations. We first revisit the time evolution of the average excess energy contained in each mode, the approach that we took in I. Figure 6 displays the results obtained in the present simulations, summarizing what was discussed in greater detail in I. In addition to the fast decay of the excited water's bend vibrational energy ($\approx$ 0.27 ps),[1,23] which as noted in the Introduction is in reasonable agreement with experimental results, the most

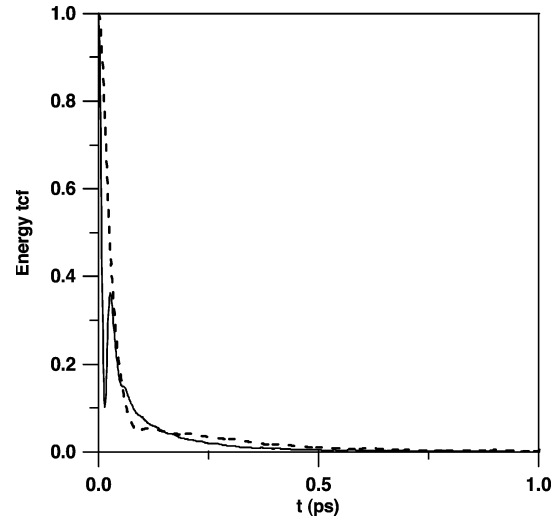

Figure 7. Normalized time correlation functions (tcfs) of H_2O rotational/translational kinetic energies, obtained from an equilibrium simulation of rigid water molecules. Continuous line: rotational energy; dashed: translational energy. The "bump" feature in the roational tcf was associated with the reversal of angular momentum in I.

remarkable aspect probably is the very modest build-up of translational/rotational energy on any of the water molecules. Obviously this does not mean that these molecular motions do not play a role, as it is clear that (with no vibrational modes available) all the energy is spread over these modes. Such small fluctuations are explained by the fact that intermolecular transfer of translational/rotational energy is substantially faster than that of vibrational energy, as was argued in I. This assertion is supported in Figure 7, which displays the time correlation functions (tcfs) of the fluctuations of translational and rotational energy (obtained from a separate equilibrium simulation with only rigid water molecules). It is easily noted by direct visual inspection (the same time span is plotted in both Figure 6 and Figure 7), that translational/rotational tcfs decay much faster than the nonequilibrium excess bend vibrational energy. Indeed, an exponential fit to both tcfs shows that their decay times are approximately 1 order of magnitude faster than the 0.27 ps characteristic of the vibrational energy. In short, even though there is initially $\approx$5 kcal/mol of excess bend vibrational energy in the central molecule, once it flows into rotational/translational energy it rapidly spreads into first neighbors and/or bulk molecules, with little build-up of excess energy in any mode. Unfortunately this makes it difficult to ascertain the specific paths through which the energy flows.

Nevertheless, and despite the high degree of noise present, the details of the excess translational/rotational energy (see inset of Figure 6), point to what mechanisms might be relevant, as discussed in I. The rise of the librational kinetic energy of the excited water molecule is the largest in amplitude and the most rapid, as is its decay, indicating that this motion is quite important in the energy flow mechanism. In comparison, for the four water neighbors, the corresponding rotational energy rise and amplitude is smaller and slightly slower respectively, with the decays also slightly slower. As for the translational energy, that of the central molecule is barely above equilibrium values, while that of its four neighbors (combined) is now slightly larger, suggesting that once rotational energy flows into translational modes the central molecule plays a role equivalent to that of its neighbors. It seems reasonable to conclude, as in I, that for the excited water bend there is an important initial energy flow to the hindered rotational motion of the bend-excited

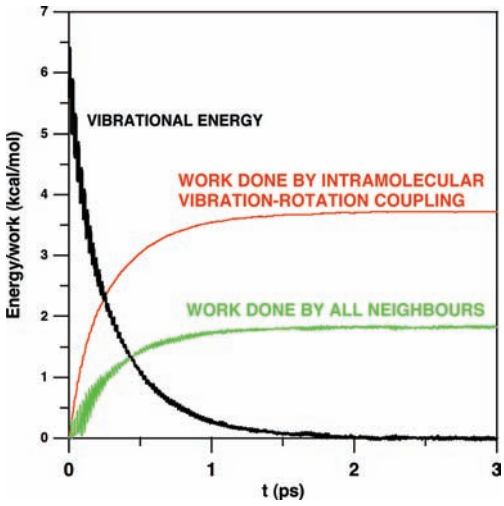

Figure 8. Basic mechanism of H_2O bend vibrational relaxation. Black: excess bend vibrational energy in the excited water molecule; red: (minus) the work performed on the water bend by centrifugal coupling (W_{VR}); green: (minus) the work performed by the excited's H_2O water neighbors (W_{ext}).

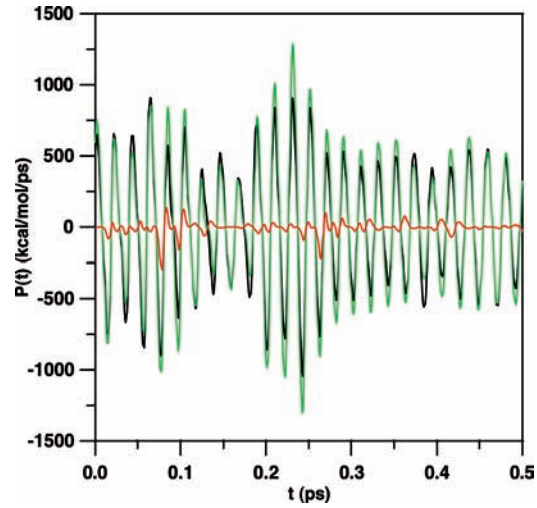

Figure 9. Contributions to the power exerted on the excited water's bend vibrational mode during a nonequilibrium trajectory. Black line: total power exerted by external forces, i.e., from all of the excited molecules's water environment, P_{vib}^{ext} (see eq 15); green: contribution to this power coming from the four closest water neighbors; red: power arising from centrifugal coupling in the bend excited water, P_{vib}^{VR} (see eq 15).

water. This librational energy, and the (predominantly first hydration shell) librational kinetic energy received directly from the excited bend, flows very rapidly through the remaining 'bulk' of the water solvent. But despite the successes of the analysis of time dependent energies in I, it is desirable to have a much more unambiguous, molecularly detailed and quantitative determination of the role played by each of the pathways sketched. We turn to this next.

C. Mechanism of Bend Relaxation. We now show that the analysis of the work and power, as described in section II, is precisely what is required to extract a clear quantitative picture of the energy flow. Figure 8 displays a core result of this work: approximately 2/3 of the excited water's excess vibrational energy goes into self-rotation through centrifugal coupling (W_{VR}, see eq 21), while the rest of the energy is transferred to the neighbors (W_{ext}), basically to the four closest waters (see below). More specifically, of the (excess) ≈5.6 kcal/mol initially put into the bending, ≈3.7 kcal/mol are transferred into its own rotation, while ≈1.8 kcal/mol is transferred to other water molecules.

Although it is true that the previous analysis of time dependent energies in I suggested an important role of centrifugal coupling, the very strong dominance just shown for this mechanism is certainly unexpected, particularly considering the balance of powers in the equilibrium simulations displayed in Figure 5. In this connection, it is interesting to note that there is no obvious change, for the power coming from different sources, during the nonequilibrium simulation. Comparison of Figures 5 and 9 (the latter obtained from a nonequilibrium trajectory) shows no fundamental differences. The direct power coming from central water's immediate neighbors still is the one that accounts for a large portion of the total power, while that coming from centrifugal coupling is much smaller. It is now clear that there is a substantial degree of cancellation when integrating the external power (to obtain the work W_{vib}^{ext}), so that comparatively little net work is done.

Returning now to Figure 8, our next step will be to provide a detailed analysis of each of the contributions in that figure. However, first we pause to examine the effect of the initial conditions. In Figure 10 we show the results obtained from simulations with the three probability distributions discussed in section III.B. Each one corresponds to a set of 500 trajectories,

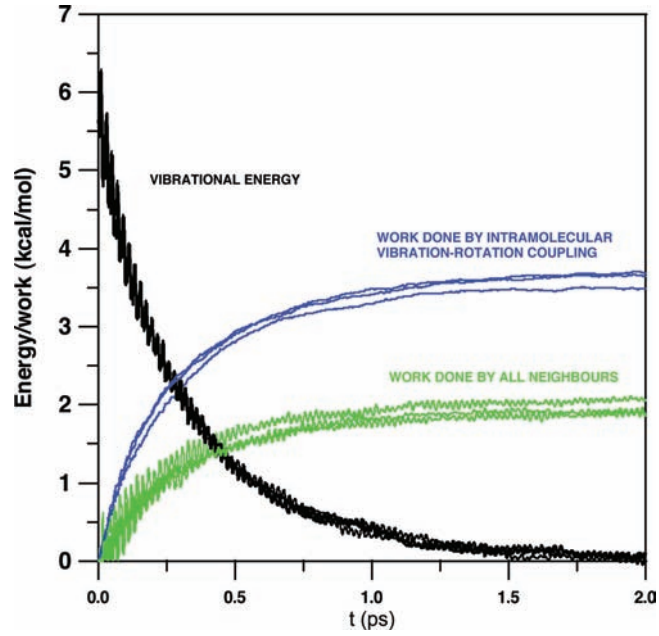

Figure 10. Results corresponding to different initial conditions (see section III.B and Figure 4). Black: excess bend vibrational energy in the excited water molecule; blue: (minus) the work performed on the water bend via centrifugal coupling (W_{VR}); green: (minus) the work performed by the excited H_2O's water neighbors (W_{ext}). The curves that slightly differ from the rest correspond to the "thermal" distribution.

of 2 ps each, with initial configurations taken 1 ps apart. The only noticeable difference is a smaller weight of centrifugal coupling in the case of the "thermal" distribution. The results are therefore rather insensitive to the sampling of initial conditions in the excited molecule.

D. Centrifugal Coupling Pathway. The importance of the VR pathway found in Figure 8 can be understood with the aid of some prior considerations. The potential effect of centrifugal coupling was discussed by Rey and Hynes in their study of vibrational relaxation of HOD in D_2O[26] using a semiclassical

approach. The general form of this coupling, applicable as well to H_2O, is

$$H_{\mathrm{Cen}} = -\frac{\hbar^{1/2}}{2}\sum_{\alpha\beta}\sum_{s}\frac{L_\alpha L_\beta}{I_\alpha I_\beta}\frac{a_s^{(\alpha\beta)}}{\omega_s^{1/2}}q_s \qquad (28)$$

where the subscripts α,β run over the three principal axes of inertia of the water molecule, I_α represents the associated moments of inertia, and L_α the corresponding angular momenta. The $a_s^{(\alpha\beta)}$ factors depend on the geometry and intramolecular potential of the molecule.[27] H_{Cen} thus shows a 2 to 1 Fermi resonance coupling between the rotational motion (L_α) and bend vibrational motion (q_s) (see also I). Of course, the same feature can be seen in the present, simpler, model (see eq 15), as the term $P_{\mathrm{vib}}^{\mathrm{VR}}$ is proportional to $\omega_\alpha{}^2$ and linear in the bending mode ($\dot{\theta}$). As a consequence, with a water bend frequency $\approx$ 1660 cm^{-1}, for H_{Cen} to be important for the relaxation process (coupled) librational modes in the neighborhood of 800 cm^{-1} are required in order to be effective. Although the peak of the H_2O librational band falls[1] at $\approx$500 cm^{-1} (if computed from the hydrogen velocity tcf), a nonnegligible contribution might exist at higher frequencies as well.

In a semiclassical approach, the rate constant for a transition between vibrational states is expressed in terms of quantum matrix elements involving the vibrational modes times the Fourier transform of the tcf of the classical degrees of freedom to which they are coupled (rotational in this case). In ref 26 Rey and Hynes showed that the relevant tcf is that of the rotational kinetic energy. This results from the observation that given the short relaxation time of the solute angular momentum in solution,[1,26] (hindered) rotation can be regarded as part of the "bath", i.e., the dynamic environment for the water bend. According to eq 28, this leads to a V-R rate constant which involves the Fourier transforms, at various frequencies, of the tcfs of various fluctuations of the bilinear rotational angular momentum terms $\delta L_\alpha L_\beta = L_\alpha L_\beta - \langle L_\alpha L_\beta\rangle$. For HOD, not all of the individual terms were examined in ref 26 but instead an approximate approach was taken in which all tcfs were approximated by the tcf of the rotational kinetic energy along a representative principal axis α (the axis perpendicular to the molecular plane, here denoted as z, was chosen in ref 26)

$$C_{\mathrm{VR}}(t) = C_{\mathrm{VR}}(t=0)\frac{\langle \delta L_\alpha^2 \delta L_\alpha^2(t)\rangle}{\langle (\delta L_\alpha^2)^2\rangle} = C_{\mathrm{VR}}(t=0)\frac{\langle \delta K_\alpha \delta K_\alpha(t)\rangle}{\langle \delta K_\alpha^2\rangle} \qquad (29)$$

where the last identity amounts to assuming that the angular momentum variable L_α is Gaussian, an assumption which turns to be rather accurate for H_2O[1] (as well as for HOD).[26] Therefore, given that the transition rate constant is proportional to the Fourier transform of $C_{\mathrm{VR}}(t)$, in the present approximation, it is the Fourier transform of the rotational kinetic energy which matters.

The above arguments, founded on a semiclassical perspective, can help to clarify the results obtained in the present work. In addition to the total molecular rotational kinetic energy tcf (Figure 7), we have also computed the tcfs of the H_2O rotational kinetic energies along each of the principal axes (see Figure 1 for the definition of axes).[28] Their Fourier transforms are displayed in Figure 11, where a vertical line signals the position

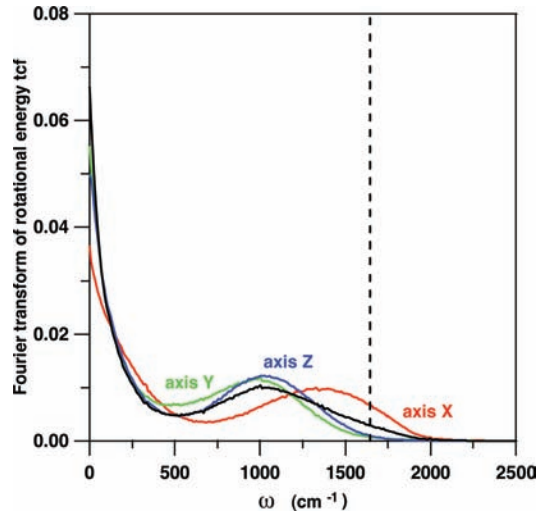

Figure 11. Fourier transform of normalized rotational kinetic energy time correlation functions for pure H_2O. The vertical dashed line denotes the water bending frequency. Black: total rotational energy; red: rotational energy with respect to body axis x (see eq 16 and Figure 1 for definitions of axes); green: same for axis y; blue: same for axis z.

of the water bending frequency. All curves decay up to $\approx$500 cm^{-1}, followed by a finite frequency maximum characteristic of the libration overtone or combination band which for the y and z axes peaks around 1000 cm^{-1}. The exception is for the x axis, for which the peak is located at $\approx$1500 cm^{-1}, which is very close to the H_2O bending transition frequency 1660 cm^{-1}, signaling a very close Fermi resonance. But as important as this 2:1 frequency matching is, it is not the only issue to be considered though, as the final outcome depends on the delicate balance of two factors, the frequency match and the coupling. First, as has just been shown, the power spectrum for the x axis is substantial at the bend frequency, while it is almost negligible for the other axes (particularly for the y axis). Second, it should be noted that the coupling itself is almost maximal for the x axis as well: according to eq 15 it is proportional to $m_O\omega_x{}^2$. This is close to the maximum coupling, which occurs for the y axis (proportional to $M\omega_y{}^2$, with $M = m_O + 2m_H$), although as noted above the power spectrum is minimal in the latter case. For the z axis, the coupling is an order of magnitude smaller (proportional to $2m_H\omega_z{}^2$) and the power spectrum is also rather small (almost identical to that of the y axis). In short, for the x axis we have substantially larger power and almost maximal VR coupling. It is the critical coincidence of both factors that makes the intramolecular energy transfer of water bend to rotation an optimal path for H_2O vibrational energy relaxation. That most of the bend energy that goes into self-rotation is actually flowing into rotation around the x axis can also be inferred from inspection of the nonequilibrium excess rotational energies around each axis, displayed in Figure 12. The excess energy for the x axis is clearly the most important, with small increases for the y axis as well and, to a slightly lesser extent, for the z axis, a pattern that reflects the balance of frequency mismatch and coupling factors just described.

E. External Work on Bending. We now discuss the other, intermolecular, channel for H_2O bend vibrational energy relaxation during the "first stage", namely the external work exerted by the rest of the liquid on the bending mode (which amounts to $\approx$1.8 kcal/mol out of the $\approx$5.6 kcal/mol of excess vibrational energy). We recall that this total work has been partitioned into three subchannels (see eq 22 and Figure 3), with the results for each one displayed in Figure 13. In contrast to

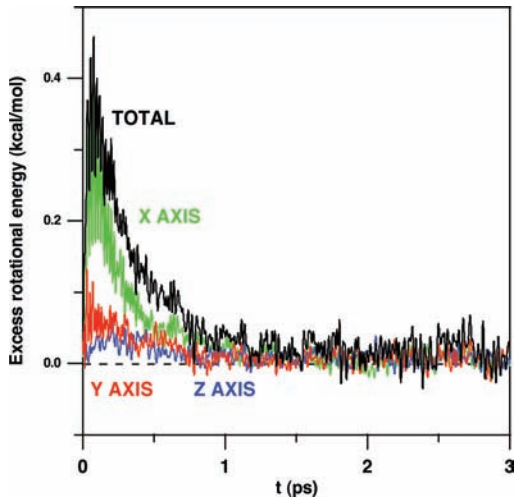

Figure 12. Excess rotational kinetic energy along each of the body centered axes of the bend vibrationally excited H_2O from nonequilibrium simulations.

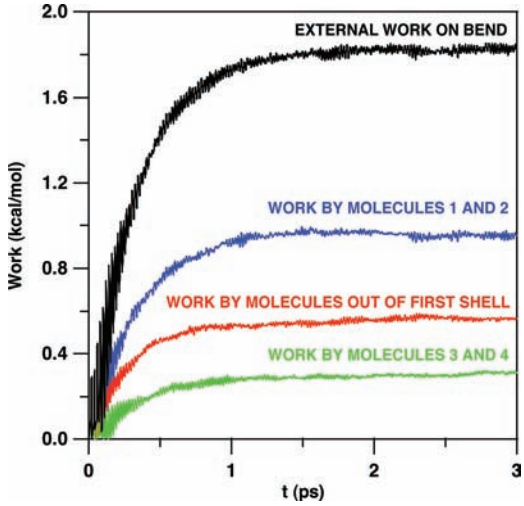

Figure 13. (Minus) the work contributions exerted by neighboring molecules on the bend of the bend-excited H_2O. See tags on each curve.

the situation for the intramolecular VR route, this time the equilibrium powers associated with the central water's immediate first hydration shell neighbors (see Figure 5) translate faithfully into the weights of different groups of molecules. The work $W_{12}^{V(C)}$ exerted by molecules 1 and 2 H-bonded to the central water's hydrogens (see Figure 2) accounts for about 50% of the total work (≈0.95 kcal/mol), while the work $W_{34}^{V(C)}$ of the H-bond donor water molecules 3 and 4 accounts for only 15% of the total work (≈0.3 kcal/mol). When taken together we see that ≈70% of the total external work is exerted by the four immediate neighbors, so that the rest of the molecules only account for ≈30% of the external work ($W_{bulk}^{V(C)} \approx 0.6$ kcal/mol) or, in other words, a 10% of the excess bend vibrational energy. The latter percentage clearly shows that the process of H_2O bend energy relaxation is basically a local one: 2/3 of the H_2O's bend energy goes intramolecularly into the water's own rotation, while the rest of the energy mainly flows into the excited water's four immediate neighbors, with only 10% of the total initial energy flowing directly into second shell molecules (and beyond).

The present results thus support an initial speculation in I. It was noted that, in the simplest image, one could imagine that the energy transfer from an excited OH bend would involve a vibration to vibration (VV) transfer from the high frequency

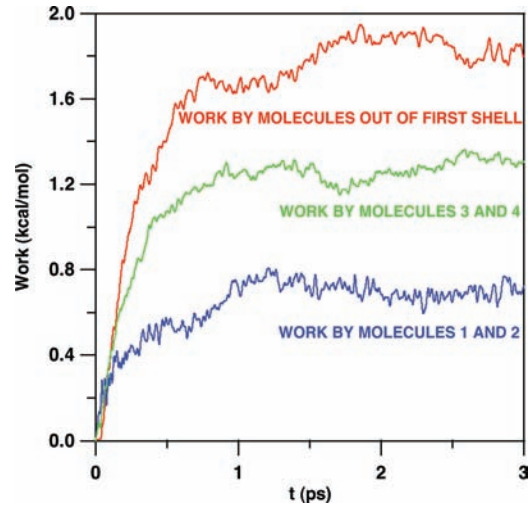

Figure 14. (Minus) the work contributions exerted by neighboring water molecules on the rotation of the bend-excited molecule. See tags on each curve.

bend to a combination or overtone of water librations. This route would necessarily involve relatively high frequency librations, and on the assumption that high frequency librations would be fairly localized, it would not involve many water molecules. It was concluded that a normal mode approach,[29] which results in at least tens of molecules involved in each mode, unfortunately did not seem to be useful in that perspective. In the present work it has been found that the basic intuition expressed in I seems correct, as bend energy goes into a very small and localized number of molecules, although it remains to be seen how this can be translated into a language involving librational modes.

F. Relaxation of Water Self-Rotation. According to the scheme in Figure 3, and in order to complete the picture of energy flow out of the initially bend excited H_2O molecule, it still remains to be seen how the energy which has flowed into self-rotation relaxes, the "second stage" in Figure 3. The external work that accounts for this flow of rotational energy is, again, partitioned into three contributions: molecules 1 and 2 ($W_{12}^{R(C)}$), molecules 3 and 4 ($W_{34}^{R(C)}$), plus the rest of the molecules outside of the first hydration shell ($W_{bulk}^{R(C)}$). The results are displayed in Figure 14: $W_{12}^{R(C)} \approx 0.7$ kcal/mol (≈15%), $W_{34}^{V(C)} \approx 1.3$ kcal/mol (≈35%), and $W_{bulk}^{R(C)} \approx 1.7$ kcal/mol (≈50%). There are several aspects to note from these ratios.

The first aspect is that almost half of the rotational energy directly goes into molecules beyond the four immediate neighbors, a pathway that accounted for only 10% of the energy flow in the case of bend vibrational energy relaxation. Therefore, while we have argued that vibrational relaxation basically is a local process, rotational relaxation is somewhat delocalized in comparison, directly reaching into water molecules that are not in direct contact with the librationally excited central water. Most probably this difference stems from the strong dipole−dipole coupling in water, leading to a more efficient transfer of rotational energy over larger separations. Here, we are referring to the classical intermolecular torque involved in this coupling, as opposed to any resonant "Förster-like" transfer, since the angular momenta are not quantized in the liquid. It is also interesting to note that the roles of molecules 1 and 2 and of molecules 3 and 4, have been almost reversed in comparison to the case of bend vibrational energy relaxation (see Figures 13 and 14). While the work done by molecules 1 and 2 on the bend vibration is three times larger than that exerted by

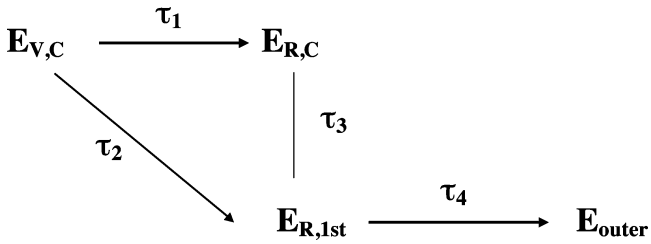

Figure 15. Simplified energy flow kinetic scheme adopted for the fitting of characteristic transition times. $E_{V,C}$, bend vibrational energy of the central H_2O molecule; $E_{R,C}$ rotational energy of that excited molecule; $E_{R,1st}$ rotational energy of first four water neighbors combined; E_{outer}, the rotational energy of the remaining waters outside the central water's first hydration shell, and translational modes of all molecules. All energies are defined as excess above the equilibrium values.

molecules 3 and 4, now we see that the work on rotation exerted by the latter is about twice that exerted by molecules 1 and 2. Again this behavior can be understood in terms of a mechanistic picture. During bend vibrational relaxation we can expect large oscillations of the bending angle, which would couple particularly strongly to the molecules H-bonded to the hydrogens (molecules 1 and 2), so that energy transfer to 1 and 2 would be more efficient than that to molecules 3 and 4. For rotational relaxation, it has been shown in section IV.D that rotational excitation of the central molecule is not isotropic, since it is mainly librational motions around axis x of the water molecule that have been rotationally excited, which involves large amplitude oscillations of the oxygen in the central water molecule. Since molecules 3 and 4 are H-bonded to that oxygen, it is to be expected that this path will now be more favorable.

V. Transition Rates and Kinetic Model

The previous discussion has been focused on the paths of energy flow out of the initially bend-excited water molecule, and on their relative weights. It is also of interest to extract the rates of energy transfer between different modes, in addition to the overall bend energy relaxation time already discussed. To this end, we will construct an approximate kinetic scheme that captures the main features of the energy flow process. The scheme adopted here is displayed in Figure 15. It contains the basic sources/sinks previously discussed: $E_{V,C}$ stands for the initial vibrational energy of the central H_2O molecule, $E_{R,C}$ for its rotational energy, $E_{R,1st}$ is the rotational energy of this water's first four neighbors combined, and E_{outer} the energy of the outer molecules, the remaining waters outside the central water's first hydration shell. All energies are defined as *excess* energies from their equilibrium values.

In this scheme, the energy flow process is pictured as one in whose first stage the initial bend vibrational energy of the central water goes into (a) its own rotation by centrifugal coupling with a time scale τ_1, and (b) to rotational energy of the four immediate water neighbors with a time scale τ_2. Note that in this accounting we are ignoring the minor channel in section IV.E that accounts for the ≈10% of the bend energy that goes directly to molecules beyond the first hydration shell.

After this initial stage, rotational energy of the central water is assumed in the second stage to go into rotations of the first water neighbors with time scale τ_3. This assumption again ignores the channel going directly to the outer neighbors, an additional ≈10% of initial bend vibrational energy. In this simplified scheme, the rotational energy of the first four water neighbors is thus channeling all the energy and finally relaxes with a time scale τ_4. Concerning this excess rotational energy of the immediate neighbors, we assume that: (a) from what we know about the relaxation of the central molecule rotation (it mainly goes to rotations of immediate neighbors), the rotational energy of the four neighbors will probably go into rotational energy of the outer water molecules, so that τ_4 should be rather similar to τ_3 although (b) when one of these four molecules relaxes, its energy goes to outer molecules and also to water molecules inside the first hydration shell, so that τ_4 should actually be slightly longer than τ_3. It should be noted that in this last stage we are ignoring energy flowing back to the first four neighbors, or from these four waters to the central water, as well as, for instance, the possibility that a rotationally excited first shell water simply exchanges with a second shell water, a process characterized by a longer time scale.[25]

What we might expect from the approximations made in our simplified scheme is that there will be more energy going into the rotation of the four neighbors than in the MD simulation, since the most drastic approximation is to neglect two energy flow channels: one that goes directly from the central water bend vibration to second shell molecules, and the one going from the rotation of the central molecule also directly to second shell. This will result in more energy being build up in rotation of the first shell waters than actually occurs. This indeed what one sees in the fit (see below); it is worse precisely for $E_{R,1st}$, with slightly higher values at initial times than the MD results.

The kinetic equations for the scheme described above are

$$\begin{aligned}
\dot{E}_{V,C} &= \left(-\frac{1}{\tau_1} - \frac{1}{\tau_2}\right)E_{V,C} \equiv -\frac{1}{\tau_{eff}}E_{V,C} \\
\dot{E}_{R,C} &= \frac{1}{\tau_1}E_{V,C} - \frac{1}{\tau_3}E_{R,C} \\
\dot{E}_{R,1st} &= \frac{1}{\tau_2}E_{V,C} + \frac{1}{\tau_3}E_{R,C} - \frac{1}{\tau_4}E_{R,1st}
\end{aligned} \tag{30}$$

whose solutions are

$$\begin{aligned}
E_{V,C}(t) &= E_0 e^{-t/\tau_{eff}} \\
E_{R,C}(t) &= E_0 \frac{\tau_3\tau_{eff}}{\tau_1(\tau_3 - \tau_{eff})}(e^{-t/\tau_3} - e^{-t/\tau_{eff}}) \\
E_{R,1st}(t) &= A\frac{\tau_4\tau_{eff}}{\tau_4 - \tau_{eff}}(e^{-t/\tau_4} - e^{-t/\tau_{eff}}) + \\
&\qquad B\frac{\tau_4\tau_3}{\tau_4 - \tau_3}(e^{-t/\tau_4} - e^{-t/\tau_3})
\end{aligned} \tag{31}$$

where we have defined

$$\begin{aligned}
A &= E_o\left(\frac{1}{\tau_2} - \frac{\tau_{eff}}{\tau_1(\tau_3 - \tau_{eff})}\right) \\
B &= E_o\frac{\tau_{eff}}{\tau_1(\tau_3 - \tau_{eff})}
\end{aligned} \tag{32}$$

Although it is possible to directly optimize the parameters in the scheme summarized by eqs 30, we follow a different route and relate, as much as possible, the different relaxation times to quantities (work contributions, effective bending relaxation time) that have already been discussed.

To this end, we start by considering that according to the kinetic scheme, the excess bend vibrational energy of the central water satisfies

$$\dot{E}_{V,C} = -\frac{1}{\tau_1}E_{V,C} - \frac{1}{\tau_2}E_{V,C} \tag{33}$$

and simultaneously must satisfy eq 20

$$\dot{E}_{V,C} = P_{vib}^{VR} + P_{vib}^{ext} = \frac{dW_{VR}}{dt} + \frac{dW_{ext}}{dt} \tag{34}$$

If we identify terms between both differential equations and substitute the time dependence of the central water bend energy from eq 31 ($E_{V,C}(t) = E_0 \exp(-t/\tau_{eff})$, which can be used to determine τ_{eff}), the following expressions result for the work contributions

$$\begin{aligned}\frac{dW_{VR}}{dt} &= -\frac{1}{\tau_1}E_{V,C} = -\frac{E_o}{\tau_1}e^{-t/\tau_{eff}} \\ \frac{dW_{ext}}{dt} &= -\frac{1}{\tau_2}E_{V,C} = -\frac{E_o}{\tau_2}e^{-t/\tau_{eff}}\end{aligned} \tag{35}$$

whose solutions are

$$\begin{aligned}W_{VR}(t) &= \frac{E_o\tau_{eff}}{\tau_1}(e^{-t/\tau_{eff}} - 1) \\ W_{ext}(t) &= \frac{E_o\tau_{eff}}{\tau_2}(e^{-t/\tau_{eff}} - 1)\end{aligned} \tag{36}$$

We pause to note the interesting feature that both work contributions have the same time scale as the relaxation of the central water bend vibrational energy (τ_{eff}). The final work contributions ($W(t\rightarrow\infty)$) are therefore

$$\begin{aligned}W_{VR} &= -\frac{E_o\tau_{eff}}{\tau_1} \\ W_{ext} &= -\frac{E_o\tau_{eff}}{\tau_2}\end{aligned} \tag{37}$$

which provides a route to extract the ratio of τ_1 and τ_2

$$\frac{\tau_1}{\tau_2} = \frac{W_{ext}}{W_{VR}} \tag{38}$$

which together with the equation that defines τ_{eff}

$$\tau_1^{-1} + \tau_2^{-1} = \tau_{eff}^{-1} \tag{39}$$

are the two equations required to obtain τ_1 and τ_2.

To summarize, in order to obtain the parameters for the kinetic scheme (eqs 30 and 31), the following procedure is followed:

• τ_{eff} is extracted from a direct fit to the decay of the central water bend vibrational energy.

• τ_1 and τ_2 are obtained from τ_{eff} and the work contribution ratio, eq 38.

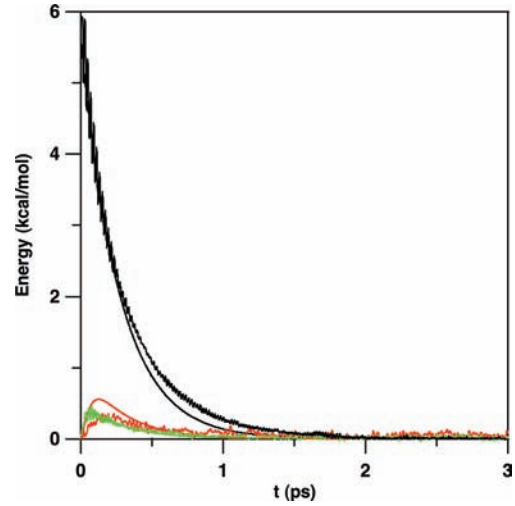

Figure 16. Fit (smooth curves) to the excess energies, for trajectories in which the bend of one of the water molecules is initially excited. Broken lines are from MD simulation (as in Figure 6). Black: vibrational energy of initially bend excited water molecule; green: rotational energy of this same molecule (note that fitted and computed curves are indistinguishable on this scale); red: rotational energy of the immediate four water neighbors combined.

• For τ_3 we use the estimation for the decay of the central water's rotational energy reported in I (≈30 fs).

• Finally, τ_4 is fine-tuned starting from a value slightly larger than τ_3, a starting point motivated by our discussion above.

The following times are obtained: $\tau_1 = 0.40$ ps, $\tau_2 = 0.82$ ps, $\tau_3 = 0.035$ ps, and $\tau_4 = 0.040$ ps. Figure 16 compares both the time evolution of the various excess energies computed with MD and the corresponding curves obtained from the simplified kinetic scheme fit. It is seen that the approximate scheme is a reasonably good description for the energy flow; as previously mentioned, the only significant disagreement is the anticipated overestimation of the four first hydration shell waters ($E_{R,1st}$), explainable in terms of our neglect of any direct flow of energy to waters in the outer shells.

VI. Concluding Remarks

In this sequel to our earlier effort,[1] we have found, via classical MD simulations and an analysis of work and power contributions, that the mechanism of the H_2O bend vibrational relaxation in liquid water is dominated by energy flow to the hindered rotation of the bend excited water molecule. This energy transfer, which represents approximately 2/3 of the transferred energy, has been analyzed as arising from a 2:1 Fermi resonance for the centrifugal coupling between the water bend and rotation. The remaining energy flow (~1/3) from the excited water bend is dominated by transfer to the excited water molecule's first four water neighbors, i.e. the first hydration shell. Approximately 3/4 of the energy flow to these neighbors is to the water molecules hydrogen (H)-bonded to the hydrogens of the central H_2O. The energy flow from the produced rotationally excited central molecule is found to be less local in character, with approximately half of its rotational kinetic energy being transferred to water molecules outside of the first hydration shell, while the remaining half, in a reversal of the behavior observed for the bend energy transfer, is preferentially (by about a factor of 2 to 1) transferred to the two first hydration shell water molecules donating H-bonds to the central water oxygen, compared to the two first hydration shell waters receiving H-bonds from this water molecule. The overall energy

flow is well described by an approximate kinetic scheme. These results strongly reinforce and greatly extend in clarity and molecular detail the results of ref 1.

A potentially important shortcoming of the present model is the lack of Coriolis coupling. This is of course the price to pay to keep the water's OH bonds fixed at their equilibrium distances, a most convenient feature in order to avoid an unphysical leak of energy from the water bend into the much higher frequency water stretches (see ref 1; see also ref 21 for an account of the difficulties involved in a classical simulation of a case where all modes are included). There are reasons to think, though, that the Coriolis coupling contribution for the water bend relaxation might be negligible. Rey and Hynes[26] showed that for HOD in D_2O the associated rate is 3 orders of magnitude smaller than the (approximate) contribution from centrifugal coupling, and six orders smaller than the one resulting from the coupling to surrounding molecules. It should be remarked that for the computation of the Coriolis coupling no approximations were required, in contrast to the case of centrifugal coupling (discussed further below). In conclusion, notwithstanding the differences between HOD and H_2O, Coriolis coupling does not seem to be a concern for bend relaxation, although it certainly might play a role for the H_2O stretch relaxation (as one can again infer from the study of HOD in D_2O).[26,30]

Another potential shortcoming is our exclusive use of a classical, rather than quantum mechanical description. While the consequences of this approximation are difficult to assess, it is noteworthy that there is a strong similarity between classical and quantum energy flow for related Fermi resonances in isolated molecule problems.[32] In addition, concerning our use of a semiclassical time correlation formula in section IV.D in the investigation of the bend−stretch Fermi resonance in connection with our nonequilibrium classical results, some justification of this argument is provided by excellent agreement found in ref 11 between nonequilibrium vibrational energy decay and a classical Landau−Teller description. In connection with the use of a classical model, the present one belongs to the group of models characterized by a decrease of the mean bending angle with respect to the gas phase, a shortcoming that could be corrected with the use of more sophisticated (polarizable) models.[33]

In the present work, for the libration of the central water we have focused on its time evolution (post energy transfer from the excited water bend) in the context of the energy flow process, and have not separately examined the nonequilibrium energy relaxation and pathway for an independently rotationally excited water, as was investigated in I. The power and work formulation employed here can also be used for the separate examination of librational excitation decay in water, a topic of independent interest.[1−3,31]

Finally, the fundamental role of centrifugal coupling found here for relaxation of the H_2O bend in pure water is in stark contrast with what was found by Rey and Hynes[26] for the bend of HOD dissolved in D_2O. There, the calculated centrifugal coupling contribution was negligible for all vibrational transitions, a result later confirmed by Lawrence and Skinner[30] in a calculation that included all terms in the centrifugal coupling. There are a number of methodological issues that might explain, in total or in part, such a disparity of results, since the theoretical approaches taken here (fully classical, with only one mode, and no approximations for the computation of the coupling) and in ref 26 (semiclassical, considering all modes, and with the somewhat strong approximations for the coupling discussed in section IV.D) are substantially different. Further, conceivably a difference in mechanism exists between H_2O and HOD. As a preliminary exploration of this issue, and in light of the crucial role that the Fourier transform of the rotational energy tcf plays in the H_2O case, we have computed the rotational kinetic energy tcfs for a HOD molecule immersed in D_2O (running a 10 ns equilibrium simulation with 108 rigid molecules). The results, displayed in Figure 17, are basically equivalent to those in Figure 11 for pure water, with just a shift to lower frequencies of about 200 cm^{-1}. According to eq 29 and the discussion of section IV.D, the importance of centrifugal coupling found in a semiclassical calculation (as the one reported in ref 26) will critically depend on which axis (α) is chosen as representative. The perpendicular z axis (see Figure 1) was chosen in ref 26 on the grounds that it is the only one that gives a nonzero contribution to Coriolis coupling. This choice, as can be seen in Figure 17, is, as was the case for H_2O in Figure 11, characterized by a minimal power at the bending frequency of HOD. If instead one would take the x axis tcf, identified in section IV.D as the key axis for the H_2O case, with a substantial power at the same frequency, we might expect a nonnegligible contribution to the relaxation. Of course the HOD couplings in this case are different than for H_2O, so that more detailed calculations and simulations are required to determine the extent of the speedup introduced (the approximate calculation in ref 26 gave the centrifugal contribution to the relaxation time on the order of a few ns). This is an open question for future work.

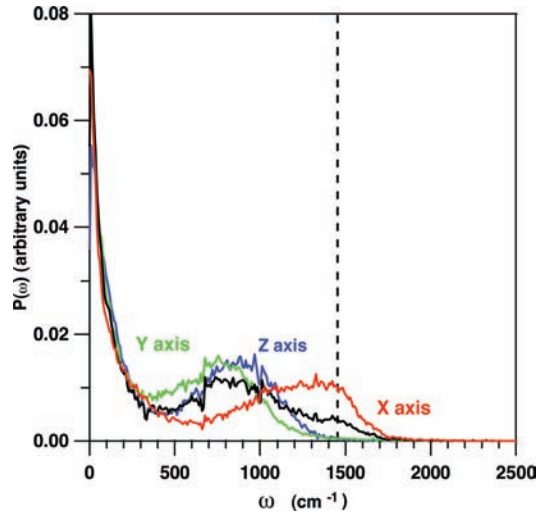

Figure 17. Fourier transform of rotational energy correlation functions for HOD in D_2O. The vertical dashed line denotes bending frequency of HOD. Black: total rotational energy; red: rotational energy with respect to body axis x (lowest inertia moment); green: same for axis y (second axis on the molecular plane); blue: same for axis z (perpendicular to molecular plane).

Note Added in Proof. A discussion of the HOD in D_2O bend relaxation has appeared, Kandratsenka, A.; Schroeder, J.; Schwarzer, D.; Vikhrenko, V. S. *J. Chem. Phys.* **2009**, *130*, 174507.

Acknowledgment. This work was supported in part by Deutsche Forschungsgemeinschaft, Sfb 450 (TE), by Project FIS2006-12436-C02-01 from MEC and Fellowship PR2008-005 from MCI (RR), and by NSF Grant CHE-0750477 (JTH).

References and Notes

(1) Ingrosso, F.; Rey, R.; Elsaesser, T.; Hynes, J. T. *J. Phys. Chem. A*, **2009**, *113*, 6657.

(2) Ashihara, S.; Huse, N.; Nibbering, E. T. J.; Elsaesser, T. *Chem. Phys. Lett.* **2006**, *424*, 66.

(3) Huse, N.; Ashihara, S.; Nibbering, E. T. J.; Elsaesser, T. *Chem. Phys. Lett.* **2005**, *404*, 389.

(4) Lindner, J.; Vohringer, P.; Pshenichnikov, M. S.; Cringus, D.; Wiersma, D. A.; Mostovoy, M. *Chem. Phys. Lett.* **2006**, *421*, 329.

(5) Lindner, J.; Cringen, D.; Pshenichnikov, M. S.; Vohringer, P. *Chem. Phys.* **2007**, *341*, 326.

(6) Kuo, C. H.; Hochstrasser, R. M. *Chem. Phys.* **2007**, *341*, 21. Chieffo, L.; Shattuck, J.; Amsden, J. J.; Eramilli, S.; Ziegler, L. D. *Chem. Phys.* **2007**, *341*, 71. These references deal with a bend-librational combination band.

(7) Raman experiments yield a longer time ∼1.4 ps: Pakoulev, A.; Wang, Z.; Pang, Y.; Dlott, D. D. *Chem. Phys. Lett.* **2003**, *380*, 404. Deàk, J. C.; Rhea, S. T.; Iwaki, L. K.; Dlott, D. D. *J. Phys. Chem. A* **2000**, *104*, 4866.

(8) This decay time of a librational excitation should be distinguished from the much longer timescale ∼1 ps on which a macroscopically heated ground state of the liquid is established by energy delocalization over many water molecules.[2,4,6]

(9) Frederick, J. H.; McClelland, G. M.; Brumer, P. *J. Chem. Phys.* **1985**, *83*, 190. Frederick, J. H.; McClelland, G. M. *J. Chem. Phys.* **1986**, *84*, 4347.

(10) (a) Kern, C. W.; Karplus, M. In *Water: A Comprehensive Treatise*; Franks, F., Ed.; Plenum: New York, 1972; Vol. 1, Chapter 2. (b) Berne, B. J.; Gordon, R. G.; Jortner, J. *J. Chem. Phys.* **1967**, *47*, 1600.

(11) (a) Whitnell, R. M.; Wilson, K. R.; Hynes, J. T. *J. Phys. Chem.* **1990**, *94*, 8625. (b) Whitnell, R. M.; Wilson, K. R.; Hynes, J. T. *J. Chem. Phys.* **1992**, *96*, 5354.

(12) Yagasaki, T.; Saito, S. *J. Chem. Phys.* **2008**, *128*, 154521.

(13) The work formulation was previously employed in connection with chemical reactions in: Gertner, B. J.; Whitnell, R. M.; Wilson, K. R.; Hynes, J. T. *J. Am. Chem. Soc.* **1991**, *113*, 74.

(14) Heidelbach, C,; Schroeder, J.; Schwarzer, D.; Vikhrenko, V. S. *Chem. Phys. Lett.* **1998**, *291*, 333. Vikhrenko, V. S.; Heidelbach, C,; Schwarzer, D.; Nemtsov, V. B.; Schroeder, J. *J. Chem. Phys.* **1998**, *110*, 5273.

(15) Berendsen, H. J. C.; Grigera, J. R.; Straatsma, T. P. *J. Phys. Chem* **1987**, *91*, 6269.

(16) Rey, R. *Chem. Phys.* **1998**, *229*, 217.

(17) Wilson, J. C.; Decius, P. C. *Molecular Vibrations*; Dover: New York, 1980.

(18) Marion, J. B.; Thornton, S. T. *Classical Dynamics of Particles and Systems*; Harcourt Brace Jovanovich: Orlando, 1988.

(19) Berendsen, H. J. C.; Postma, J. P. M.; van Gunsteren, W. F.; DiNola, A.; Haak, J. R. *J. Chem. Phys.* **1984**, *81*, 3684.

(20) Ryckaert, J. P.; Ciccotti, G.; Berendsen, H. J. C. *Comp. Phys.* **1977**, *23*, 327.

(21) Ramesh, S. G.; Sibert, E. L. *J. Chem. Phys.* **2006**, *125*, 244516.

(22) Andersen, H. C. J. *Comp. Phys.* **1983**, *52*, 24.

(23) The present results are well described at short times by a 270 fs relaxation time (see below). This is the same time reported in I and will be used in the following discussion. We note though that for time intervals larger than 0.5 ps, a value of 300 fs provides a better fit. This small difference between the independent simulations reported here and I seems reasonable considering the different sampling of initial conditions and integration algorithms, providing an estimate of the statistical dispersion that might be expected.

(24) Goldstein, H. *Classical Mechanics*; Addison-Wesley: Reading, MA, 1980.

(25) Laage, D.; Hynes, J. T. *J. Phys. Chem. B* **2008**, *112*, 7697.

(26) Rey, R.; Hynes, J. T. *J. Chem. Phys.* **1996**, *104*, 2356.

(27) See ref 10a.

(28) As noted in I, an Instantaneous Normal Mode Approach[29] might well be instructive for these tcfs and their Fourier transforms.

(29) Cho, M.; Fleming, G. R.; Saito, S.; Ohmine, I.; Stratt, R. M. *J. Chem. Phys.* **1994**, *100*, 6672.

(30) Lawrence, C. P.; Skinner, J. L. *J. Chem. Phys.* **2002**, *117*, 5827.

(31) Saito, S.; Ohmine, I. *J. Chem. Phys.* **2006**, *125*, 084506.

(32) Sibert, E. L., III.; Hynes, J. T.; Reinhardt, W. P. *J. Chem. Phys.* **1984**, *81*, 1135. Sibert, E. L., III.; Reinhardt, W. P.; Hynes, J. T. *J. Chem. Phys.* **1984**, *81*, 1115.

(33) Fanourgakis, G. S.; Xantheas, S. S. *J. Chem. Phys.* **2006**, *124*, 174504.

JP9036342